

**DEVELOPMENT AND INVESTIGATION OF
ATMOSPHERIC PRESSURE NON-THERMAL
RF PLASMA JET**

MAHREEN



DEPARTMENT OF ENERGY SCIENCE AND ENGINEERING

INDIAN INSTITUTE OF TECHNOLOGY DELHI

JANUARY 2023

©Indian Institute of Technology Delhi (IITD), New Delhi, India, 2023

**DEVELOPMENT AND INVESTIGATION OF
ATMOSPHERIC PRESSURE NON-THERMAL
RF PLASMA JET**

By

Mahreen

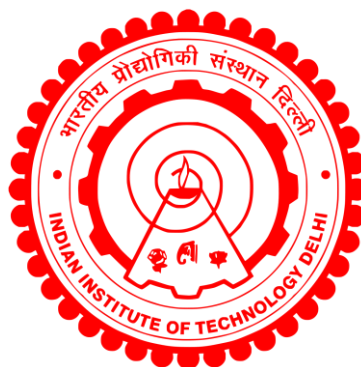
(2017ESZ8210)

Department of Energy Science and Engineering

Submitted

in partial fulfillment of the requirements for the degree of

DOCTOR OF PHILOSOPHY



to

INDIAN INSTITUTE OF TECHNOLOGY DELHI

JANUARY 2023

*Dedicated to my
Family...*

UNDERTAKING

I hereby declare that the work presented here in the thesis has been carried out by me towards the partial fulfilment of the requirement for the award of the degree of **Doctor of Philosophy** at the Indian Institute of Technology Delhi. The content of this report, in full or in parts, have not been submitted to any other institute or university for the award of any degree.

Mahreen

Name: Mahreen

Entry number: 2017ESZ8210

Email id.: esz178210@dese.iitd.ac.in

CERTIFICATE

This is to certify that the thesis entitled, “**Development and Investigation of Atmospheric Pressure Non-Thermal RF Plasma Jet**”, submitted by **Ms. Mahreen**, to the Indian Institute of Technology, Delhi for the award of the degree of **Doctor of Philosophy**, is a bonafide record of the research work done by her under our supervision.

In my opinion, the thesis has reached the standard of fulfilling the requirement of all the regulations regarding the degree. The results contained in this thesis have not been submitted, in part or in full, to any other university or institute to award any degree or diploma.

Satyananda Kar
Prof. Satyananda Kar

Department of Energy Science
and Engineering
IIT Delhi, New Delhi, India

Debaprasad Sahu

Prof. Debaprasad Sahu
Department of Energy Science
and Engineering
IIT Delhi, New Delhi, India

Acknowledgements

I express my gratefulness to the Almighty for enabling me to complete my thesis. This thesis becomes a reality with the kind support of many individuals and my sincere thanks to all of them.

First and foremost, I express my profound gratitude to my research supervisors **Prof. Satyananda Kar** and **Prof. Debaprasad Sahu** for giving me the opportunity to perform research and providing invaluable guidance throughout my Ph.D. Their patience, humbleness and encouragement have enabled me to complete my thesis. I appreciate the confidence they have always shown in me.

With a great sense of gratitude, I would like to thank **Prof. Ashish Ganguli**. His dynamism, vision and motivation have deeply inspired me and it was a great privilege to learn the research methodology under his guidance. His enthusiasm and love for research are unmatched and it would not be possible without his supervision to shape the ideas into real research problems.

I am also grateful to my research committee members: **Prof. Ramesh Narayanan**, **Prof. P. Senthilkumaran** and **Prof. K. A. Subramanian**, for their continued support and encouragement. A special thanks to **Prof. Ramesh Narayanan** for sharing his knowledge and giving me valuable advice during this entire period. It is my honour to thank **Prof. R. D. Tarey** for his priceless technical suggestions during the development of the experimental system. I am also thankful to **Prof. Sumit K Chattopadhyay** for helping me in setup the calibration procedure for an important part of the experimental system.

My earnest acknowledgement to **Dr. G. Veda Prakash** for his constant guidance and support for the complete duration of Ph.D. He made himself available for planning, building and improving the experimental setups and was always enthusiastic to work on the challenges that I have ever faced. I relish the on- and off-topic discussions with him which greatly increased the quality of this work.

I thank **Mr. A. J. Josekutty** for his valuable and constructive suggestions during the planning and development of experimental work in the initial phase of Ph.D. I am also thankful

to **Mr. Has Mukh Kabariya** for helping me to develop an electronic circuit for my experiments. I am very much thankful to the MHRD, India for the Ph.D. scholarship.

Special thanks go to my fellow labmates and friends: **Dr. Arti Sarawal, Dr. Anshu Verma, Dr. Prashant K Barnwal, Ms. Priti Singh, Ms. Shweta Sharma, Mr. Aishik Basu Mallick, Mr. Sarthak Das, Ms. Radhika T P, Mr. Tejaswi Rana, Ms. Pragya Joshi, Ms. Anuravi Sharma** and all the new members of Plasma Physics Laboratory for being the part of my Ph.D journey. I thank **Dr. Anshu Verma** and **Dr. Arti Rawat** for making themselves available for the discussions and sharing their experiences of subjects. A special thanks to my friend **Shweta**, for her advice and care, and for bracing me during difficult situations. I would like to thank my all-time friend **Mr. Kiran Kumar N** and my friends at the IITD hostel, **Dr. Alka Jakhar** and **Ms. Shayesta Wajid** for their support and encouragement during the hard times.

Last but not the least, I am thankful to my family for their love, prayers, care and sacrifices in educating and preparing me for my future. Words fail to express my heartfelt gratitude to my grandfather **Mr. Rafi Khan**, my father **Mr. Shareef Khan**, my mother **Mrs. Seema Yasmeen**, my siblings **Mahak Khan** and **Humair Khan**, and my brother-in-law **Mr. Asif** for their moral support and encouragement.

Mahreen

Abstract

Non-thermal Atmospheric Pressure Plasma Jets (APPJs) are popular for the generation of various chemically activated species in ambient air. In interaction with the target, these species participate in a variety of favourable chemical reactions suitable for several industrial and biomedical applications. In this context, an accurate estimation of plasma parameters alleviates the optimization of plasma jets for applications. However, the realization of control and optimization of plasma jets for specific applications has a long way to go still, specifically for RF APPJ, where high frequencies introduce additional complexities in plasma diagnostics and source optimization. All this, therefore, necessitates an in-depth understanding of the APPJs and the influence of operating parameters on their characteristics.

In this thesis, a 13.56 MHz RF-based APPJ was designed and fabricated to investigate its characteristics under various operating conditions using argon and helium as feed gases. To boost the open circuit voltage at the plasma terminals and aid discharge initiation at low input powers (~ 2 W), an indigenously developed LC series resonant circuit is used in *between* the matching network and the APPJ device. This thesis reports a theoretical and experimental investigation on helium and argon plasma discharges in the RF APPJ in continuous wave (CW) and pulse modulation (PM) mode. Various diagnostic tools like electrical (V-I) probes, optical imaging, emission spectra, and thermal and acoustic measurements were employed extensively for the characterization of the APPJ.

The operation of APPJ in PM mode offered a lower gas temperature suitable for certain applications and revealed several unique characteristics of helium APPJ. To effectively describe the plasma features as a function of the modulating frequency (50 Hz -10 kHz), duty cycle (10-80%) and RF input power (10- 50 W) etc., a detailed and systematic study was performed on the PM helium APPJ. This study investigated the influence of RF modulation frequency on helium APPJ's fundamental characteristics i.e., discharge behavior, plasma dimensions, generation of reactive species, and the basic plasma parameters including electron density (n_e), electron excitation temperature (T_{exc}), and gas temperature (T_g). From the experiments, it was observed that operating the plasma jet at low pulse modulation frequencies (around 50 Hz) provides enhanced plasma dimensions (longer and more homogeneous plasma plume), higher electron

density and increased reactive species (viz., He I, O, OH, N_2^+ , etc.) as compared to operation at higher modulation frequencies.

On the other hand, a plasma jet operated in PM mode with argon produced a novel helical shape APPJ, which is very different from the conventional smooth conical shape. In particular, this helical shape was observed when operated around ~ 2 kHz RF pulse modulation frequency, $\sim 30\%$ duty cycle, ~ 50 W applied power and ~ 1.5 lpm argon gas flow rate. It is most likely that the helical shape in argon APPJ originated due to periodic heating and cooling of the gas triggered by repetitive application of RF pulses, which imparted periodic thrusts to gas and plasma that can *excite sound or ion acoustic waves* with non-zero azimuthal mode number (that can be shown to *carry orbital angular momentum* as well) in the plasma-gas mix. It is also possible for the electrostatic sound waves with orbital angular momentum to allow the formation of a helical-shaped jet. A physical model (along the above lines) attempting the origin of the helical shape of the APPJ is proposed along with a thorough experimental investigation to identify the operational parameter regime of the helical shape by employing a wide range of operating parameters.

Electrical diagnostics (voltage and current probes) are commonly used to estimate power dissipation in most conventional plasma loads. However, the use of standard Voltage (V) and current (I) probes with miniature devices like RF APPJs yields highly uncertain electrical characterization on account of the latter's highly capacitive nature of the sheaths at the electrodes. Consequently, one has a very ambiguous estimation of the RF power fed to the APPJ and hence, its plasma parameters. For accurate estimation of the electrical, and plasma parameters, a new calibration technique is conceptualized for V-I probes which avoided the measurement errors in amplitude and phase while utilizing them at RF APPJs. The calibration procedure involves generating a new set of calibration constants for the two probes from which one may determine the true voltage, V_t and the true current, I_t . Following the joint calibration of the probes, the V-I probe measurements yield fairly accurate and reliable estimates of the different electrical metrics like the average power absorbed by the plasma, the complex plasma impedance, forward and reflected wave amplitudes, etc. However, to estimate the plasma density (n), electron temperature (T_e) and other relevant parameters of the APPJ a model of the discharge region of the APPJ device is needed. The only input to such a model apart from the

geometry of the device and the feed gas would be the power fed to the APPJ, which can be provided from the V-I probe measurements.

To support and augment the electrical measurements discussed above, an analytical, 2-D model for the APPJ's discharge region (inside the glass tube) is developed in this thesis. The model takes into account the gas flow and it is based on particle and power balance equations. It determined the radial and axial variations of plasma density (n), axial and radial fluxes, electron temperature (T_e), gas temperature (T_g) and the total plasma and power flowing out of the discharge region with power fed to the discharge being given by the V-I measurement data. Typically, n is found to be $\approx 3.9 \times 10^{17} \text{ m}^{-3}$ and $\approx 2.8 \times 10^{19} \text{ m}^{-3}$ and T_e found to be $\approx 1.8 \text{ eV}$ and $\approx 0.8 \text{ eV}$ at 25 W of RF power for helium and argon plasma, respectively.

सार

गैर-थर्मल वायुमंडलीय दबाव प्लाज्मा जेट (APPJ) परिवेशी वायु में विभिन्न रासायनिक रूप से सक्रिय प्रजातियों की पीढ़ी के लिए लोकप्रिय हैं। लक्ष्य के साथ बातचीत में, ये प्रजातियां कई औद्योगिक और जैव चिकित्सा अनुप्रयोगों के लिए उपयुक्त विभिन्न प्रकार की अनुकूल रासायनिक प्रतिक्रियाओं में भाग लेती हैं। इस संदर्भ में, प्लाज्मा मापदंडों का सटीक अनुमान अनुप्रयोगों के लिए प्लाज्मा जेट के अनुकूलन को कम करता है। हालांकि, विशिष्ट अनुप्रयोगों के लिए प्लाज्मा जेट के नियंत्रण और अनुकूलन की प्राप्ति के लिए अभी भी एक लंबा रास्ता तय करना है, विशेष रूप से आरएफ APPJ के लिए, जहां उच्च आवृत्तियां प्लाज्मा डायग्नोस्टिक्स और स्रोत अनुकूलन में अतिरिक्त जटिलताओं का परिचय देती हैं। इसलिए यह सब, APPJ की गहन समझ और इसकी विशेषताओं पर ऑपरेटिंग मापदंडों के प्रभाव की आवश्यकता है।

इस थीसिस में, एक 13.56 मेगाहर्ट्ज RF का उपयोग APPJ को डिजाइन और निर्माण करने के लिए किया जाता है ताकि विभिन्न ऑपरेटिंग परिस्थितियों में आर्गन और हीलियम का उपयोग फ्रीड गैसों के रूप में इसकी विशेषताओं की जांच की जा सके। प्लाज्मा टर्मिनलों पर ओपन सर्किट वोल्टेज को बढ़ावा देने और कम इनपुट पावर (~ 2 W) पर डिस्चार्ज दीक्षा में सहायता के लिए, स्वदेशी रूप से विकसित LC सीरीज रेजोनेंट सर्किट का उपयोग मिलान नेटवर्क और APPJ डिवाइस के बीच किया जाता है। यह थीसिस निरंतर तरंग (CW) और पल्स मॉड्यूलेशन (PM) मोड में RF APPJ में हीलियम और आर्गन प्लाज्मा डिस्चार्ज पर सैद्धांतिक और प्रयोगात्मक जांच की रिपोर्ट करती है। APPJ के लक्षण वर्णन के लिए विद्युत (V-I) जांच, ऑप्टिकल इमेजिंग, उत्सर्जन स्पेक्ट्रा, थर्मल और ध्वनिक माप जैसे विभिन्न नैदानिक उपकरण बड़े पैमाने पर कार्यरत हैं।

PM मोड में APPJ के संचालन ने कुछ अनुप्रयोगों के लिए उपयुक्त कम गैस तापमान की पेशकश की और हीलियम APPJ की कई अनूठी विशेषताओं का खुलासा किया। पीएम हीलियम APPJ में मॉड्यूलेटिंग आवृत्ति (50 Hz-10 kHz), ड्यूटी चक्र (10- 80%) और आरएफ इनपुट पावर (10- 50 W) आदि के एक समारोह के रूप में प्लाज्मा सुविधाओं का प्रभावी ढंग से वर्णन करने के लिए, एक विस्तृत और व्यवस्थित अध्ययन किया गया था। यह अध्ययन हीलियम APPJ की मूलभूत विशेषताओं यानी डिस्चार्ज व्यवहार, प्लाज्मा आयाम, प्रतिक्रियाशील प्रजातियों की पीढ़ी और इलेक्ट्रॉन घनत्व (n_e), इलेक्ट्रॉन उत्तेजना तापमान (T_{exc}), और गैस तापमान सहित बुनियादी प्लाज्मा मापदंडों पर आरएफ मॉड्यूलेशन आवृत्ति के

प्रभाव की जांच करता है। प्रयोगों से, यह देखा गया कि उच्च मॉड्यूलन आवृत्तियों पर संचालन की तुलना में कम पल्स मॉड्यूलेशन आवृत्तियों (लगभग 50 Hz) पर प्लाज्मा जेट को संचालित करने से प्लाज्मा आयाम (लंबे और अधिक सजातीय प्लाज्मा प्लम), उच्च इलेक्ट्रॉन घनत्व और बढ़ी हुई प्रतिक्रियाशील प्रजातियां (जैसे, He I, O, OH, N₂⁺, etc) आदि प्रदान करती हैं।

दूसरी ओर, आर्गन के साथ पीएम मोड में संचालित एक प्लाज्मा जेट ने एक उपन्यास पेचदार आकार APPJ का उत्पादन किया, जो पारंपरिक चिकनी शंकाकार आकृति से बहुत अलग है। विशेष रूप से, यह पेचदार आकार तब देखा जाता है जब ~ 2 kHz RF पल्स मॉड्यूलेशन आवृत्ति, ~ 30% ड्यूटी चक्र, ~ 50 W इनपुट पावर और ~ 1.5 lpm आर्गन गैस प्रवाह दर के आसपास संचालित होता है। यह सबसे अधिक संभावना है कि आर्गन APPJ में पेचदार आकार आरएफ दालों के दोहराव वाले अनुप्रयोग द्वारा ट्रिगर गैस के आवधिक हीटिंग और कूलिंग के कारण उत्पन्न होता है, जो गैस और प्लाज्मा को आवधिक जोर देता है जो गैर-शून्य अज़ीमुथल के साथ ध्वनि या आयन ध्वनिक तरंगों को उत्तेजित कर सकता है। प्लाज्मा-गैस मिश्रण में मोड संख्या (जिसे कक्षीय कोणीय गति को भी ले जाने के लिए दिखाया जा सकता है)। कक्षीय कोणीय गति के साथ इलेक्ट्रोस्टैटिक ध्वनि तरंगों के लिए एक पेचदार आकार के जेट के गठन की अनुमति देना भी संभव है। APPJ के पेचदार आकार की उत्पत्ति का प्रयास करने वाला एक भौतिक मॉडल (उपरोक्त पंक्तियों के साथ) ऑपरेटिंग मापदंडों की एक विस्तृत श्रृंखला को नियोजित करके पेचदार आकार के परिचालन पैरामीटर शासन की पहचान करने के लिए एक गहन प्रयोगात्मक जांच के साथ प्रस्तावित है।

विद्युत निदान (V-I जांच) का उपयोग आमतौर पर अधिकांश पारंपरिक प्लाज्मा भारों में बिजली अपव्यय का अनुमान लगाने के लिए किया जाता है। हालांकि, आरएफ APPJ जैसे लघु उपकरणों के साथ मानक वोल्टेज (V) और वर्तमान (I) जांच का उपयोग इलेक्ट्रोड पर म्यान की अत्यधिक कैपेसिटिव प्रकृति के कारण APPJ के अत्यधिक अनिश्चित विद्युत लक्षण वर्णन करता है। नतीजतन, किसी के पास APPJ को खिलाई गई आरएफ शक्ति का बहुत अस्पष्ट अनुमान है और इसलिए, इसके प्लाज्मा पैरामीटर। विद्युत, प्लाज्मा मापदंडों के सटीक आकलन के लिए, V-I जांच के लिए एक नई अंशांकन तकनीक की अवधारणा की गई है जो आरएफ APPJ में उनका उपयोग करते समय आयाम और चरण में माप त्रुटियों से बचाती है। अंशांकन प्रक्रिया में दो जांचों के लिए अंशांकन स्थिरांक का एक नया सेट उत्पन्न करना शामिल है जिससे कोई वास्तविक वोल्टेज, V_r और वास्तविक वर्तमान, I_r निर्धारित कर सकता है। जांच के संयुक्त अंशांकन के

बाद, V-I जांच माप विभिन्न विद्युत मेट्रिक्स के काफी सटीक और विश्वसनीय अनुमान प्राप्त करते हैं जैसे प्लाज्मा द्वारा अवशोषित औसत शक्ति, जटिल प्लाज्मा प्रतिबाधा, आगे और परावर्तित तरंग आयाम, आदि। हालांकि, क्रम में करने के लिए APPJ के प्लाज्मा घनत्व, इलेक्ट्रॉन तापमान और अन्य प्रासंगिक मापदंडों का अनुमान लगाएं, APPJ डिवाइस के निर्वहन क्षेत्र के एक मॉडल की जरूरत है। ऐसे मॉडल का एकमात्र इनपुट, डिवाइस की ज्यामिति और फीड गैस के अलावा APPJ को दी जाने वाली शक्ति होगी, जिसे V-I जांच माप से प्रदान किया जा सकता है।

विद्युत माप को समर्थन और बढ़ाने के लिए ऊपर चर्चा की गई, इस थीसिस में पहली बार APPJ के निर्वहन क्षेत्र (ग्लास ट्यूब के अंदर) के लिए एक विश्लेषणात्मक, 2-डी मॉडल विकसित किया गया है। मॉडल गैस प्रवाह को ध्यान में रखता है और कण और शक्ति संतुलन समीकरणों पर आधारित है। यह प्लाज्मा घनत्व (n), अक्षीय और रेडियल प्रवाह, इलेक्ट्रॉन तापमान (T_e), गैस तापमान (T_g) के रेडियल और अक्षीय विविधताओं को निर्धारित करता है और निर्वहन क्षेत्र से बहने वाली कुल प्लाज्मा और शक्ति को खिलाती है। डिस्चार्ज V-I माप डेटा द्वारा दिया जा रहा है। आमतौर पर, हीलियम और आर्गन प्लाज्मा के लिए $n \approx 3.9 \times 10^{17} \text{ m}^{-3}$ और $\approx 2.8 \times 10^{19} \text{ m}^{-3}$ और $T_e \approx 1.8 \text{ eV}$ और $\approx 0.8 \text{ eV}$ 25 क्रमशः पाया जाता है।

Table of Contents

Certificate	i
Acknowledgements	iii
Abstract	v
List of Content	xiii
List of Figures	xvii
List of Tables	xxi
List of Abbreviations	xxiii
List of Notations	xxv
Chapter	
1. Introduction	1
1.1 Non-thermal atmospheric pressure plasma	2
1.2 Challenges to generate atmospheric pressure non-thermal plasma.....	5
1.3 Atmospheric pressure non-thermal plasma sources	6
1.4 Radio Frequency Atmospheric Pressure Plasma Jet (RF-APPJ)	10
1.5 Literature survey	15
1.5.1 Characteristics of pulse modulated RF APPJ	15
1.5.2 Unconventional shape of APPJ.....	18
1.5.3 Electrical characterization and theoretical modelling of RF APPJ.....	19
1.6 Research plan	21
1.6.1 Research gaps in literature	21
1.6.2 Formulation of research objectives.....	25
1.7 Outline of thesis	27
2. Experimental Setup and Diagnostics	29
2.1 Development of the RF Atmospheric Pressure Plasma Jet (RF-APPJ)	30
2.2 Diagnostics	36
2.2.1 Voltage and Current (V-I) Probes.....	37

2.2.2	Optical Emission Spectroscopy (OES)	39
2.2.3	High-speed camera.....	49
2.2.4	K-type thermocouple	50
2.2.5	Microphone	50
2.3	Summary	51
3.	Characteristics of pulse modulated helium RF atmospheric pressure plasma jet	53
3.1	Introduction	54
3.2	Motivation for using low modulation frequency in pulsed RF APPJs.....	55
3.3	Pulse Modulated Helium Plasma Jet.....	56
3.4	Experimental observations and analysis	58
3.4.1	Influence of modulation frequency.....	58
3.4.2	Fixed average power for CW and PM modes.....	69
3.4.3	Influence of duty cycle.....	70
3.4.4	Influence of RF input power	74
3.5	Summary	76
4.	Excitation and analysis of helical shape argon atmospheric pressure plasma jet using RF pulse modulation.....	79
4.1	Generation of helical-shaped plasma jet	80
4.2	Understanding the characteristics of helical shape APPJ.....	84
4.2.1	Geometrical features of the helical plasma jet.....	84
4.2.2	Emission spectra and plasma parameter estimation of helical APPJ.....	85
4.2.3	Mechanism of helical plasma jet formation.....	86
4.3	Parametric analysis and Discussion	91
4.3.1	Effect of duty cycle.....	91
4.3.2	Effect of modulation frequency	97
4.3.3	Effect of gas flow rate.....	99
4.3.4	Effect of input RF power	102
4.4	Comparison between helium and argon plasma jet.....	103
4.5	Summary	106
5.	Analysis and Characterization of RF APPJ Using a 2-D Plasma Jet Model and Jointly Calibrated V-I Probes.....	109

5.1	Introduction	110
5.2	Joint calibration of V-I probes	111
5.2.1	Joint calibration procedure.....	111
5.2.2	Verification of joint calibration efficacy.....	114
5.2.3	Transformation of Vt and It to APPJ terminals.....	117
5.3	A two-dimensional model for plasma jet.....	119
5.3.1	The geometry of the model.....	119
5.3.2	RF power absorption mechanism in APPJ.....	120
5.3.3	The APPJ model	124
5.4	Results and discussion.....	136
5.4.1	Outcomes of the APPJ model	136
5.4.2	OES analysis	142
5.4.3	Pulsed operation.....	135
5.5	Summary	143
6.	Conclusions and Future Scope	145
6.1	Summary of the thesis	146
6.2	Prospects for future research.....	148
	Appendix (A-1)	151
	Appendix (A-2).....	153
	References.....	155
	Biodata.....	169

List of Figures

Figure 1.1 : Schematic illustration of selected applications of atmospheric pressure non-thermal plasma	4
Figure 1.2: (a) Breakdown potential in various gases (b) electron and gas temperature as a function of pressure.....	6
Figure 1.3: Sources for atmospheric pressure non-thermal plasma generation.....	7
Figure 1.4: Breakdown voltage as a function of frequency relative to its DC value.....	12
Figure 2.1: Schematic of atmospheric pressure RF plasma jet system.....	30
Figure 2.2: L-type Matching Network (MN) used for impedance matching.....	31
Figure 2.3: (a) Layout of the resonance circuit (b) photograph of resonance circuit.....	32
Figure 2.4: Cross-field configuration of the APPJ along with dimensions (a) front view (b) bottom view	34
Figure 2.5: (a) Schematic of APPJ assembly (b) Photographs of the plasma jet assembly	36
Figure 2.6: Images of high voltage probe and current probe.....	37
Figure 2.7: Two locations for placement of voltage and current probes	39
Figure 2.8: (a) Position of tip of optical fiber (b) Typical emission spectra of helium APPJ.....	41
Figure 2.9: Typical Boltzmann plot for estimation of T_{exc} for helium plasma jet	43
Figure 2.10: Spectrum fitting of the experimental OH band by Lifbase simulation spectra.....	45
Figure 2.11: Voigt fitting of typical H_{β} line for electron density measurement	46
Figure 2.12: Photograph of Phantom VEO 410 high speed camera.....	50
Figure 3.1: Typical RF voltage waveform pulse modulated at 50 Hz modulation frequency.....	56
Figure 3.2: (a) Frontal images of APPJ in CW and PM (b) Discharge images (c) Length and width of plasma.....	59
Figure 3.3: Plasma gas temperature variation with RF power for CW and PM mode	62

Figure 3.4: (a) OES of atmospheric pressure helium APPJ in PM mode (b) Normalized intensities of helium line (706 nm), (c) OH line (309 nm) N ₂ and N ₂ ⁺ lines, O line (777.4 nm) for various modulation frequencies.	65
Figure 3.5: Typical Boltzmann plot fitting for electron excitation temperature.....	66
Figure 3.6: Normalized spectra line H _β and corresponding Voigt-function fitting	67
Figure 3.7: The variation of T_{exc} and n_e with reference to the modulation frequency.	68
Figure 3.8: (a) Images of APPJ in CW and PM modes at 15 W average power (b) Intensity comparison of plasma emission in CW and PM modes at 15 W average power.	69
Figure 3.9: (a) Images of helium plasma jet as a function of duty cycle.....	71
Figure 3.10: Images for fixed average RF power (15 W) with variation in duty cycle.....	73
Figure 3.11: Images of helium plasma jet as a function of applied power	74
Figure 3.12: (a) Plasma jet dimension variation (b) RONS intensity variation with RF power. 75	75
Figure 4.1: Schematic of the experimental setup used for pulse-modulated RF argon APPJ.. ...	80
Figure 4.2: Schematic showing the two camera arrangements: (a) front view (b) tilted view. ..	81
Figure 4.3: Typical 2D images of a plasma jet in ambient air. (a) CW mode (b) PM mode	82
Figure 4.4: High speed images of helical shape APPJ at different exposure time of camera	83
Figure 4.5 : (a) Shows the location of the plasma bending (b) Spatial intensity of the APPJ	84
Figure 4.6: Time integrated emission spectra of argon pulse modulated RF plasma jet.....	86
Figure 4.7: Typical waveform of pulse-modulated RF voltage.....	87
Figure 4.8: Frequency spectrum of the measured acoustic signal	89
Figure 4.9: Pictorial representation of propagating helical APPJ with right-handed OAM.....	90
Figure 4.10: Effect of pulse duty cycle on plasma jet shape	92
Figure 4.11: Effect of duty cycle on plasma jet length and plasma width at the nozzle.	94
Figure 4.12: Effect of pulse duty cycle on plasma jet shape at fixed average power.....	95
Figure 4.13: Measured APPJ length at various duty cycles by keeping average power fixed	96

Figure 4.14: 2D front view images of pulse modulated RF plasma jet under different modulation frequencies	97
Figure 4.15: Effect of modulation frequency on the properties of pulse modulated RF APPJ ...	98
Figure 4.16: Images of helical plasma jet as a function of the argon gas flow rate.....	100
Figure 4.17: Plasma jet length as a function of argon gas flow rate.....	101
Figure 4.18: Effect of RF power on the helical shape of plasma jet.....	102
Figure 4.19: Variation of plasma jet length and width as a function of power	103
Figure 4.20: Comparison of the shape of the plasma jet in CW mode (a) argon (b) helium	104
Figure 4.21: Comparison of the shape of the plasma jet in pulse modulation mode.....	105
Figure 5.1: The scheme for V-I probe arrangement and joint calibration	112
Figure 5.2: Geometrical view of the RF plasma jet discharge regions used to develop a theoretical model.....	119
Figure 5.3: Electric field configuration of RF plasma jet discharge regions.	123
Figure 5.4: Plot of radial function $-R/A$	129
Figure 5.5: Spatial variation of plasma density in He APPJ.....	138

List of Tables

Table 1.1: Temperature difference of thermal and non-thermal plasma.....	2
Table 2.1: Details of the OES systems used in experiment	40
Table 2.2: Excitation energy and transition strength at observed wavelengths of helium.....	42
Table 2.3: Details of the different broadening mechanisms in atmospheric pressure plasma	48
Table 4.1: Average power, pulse duration and gas temperature with reference to the duty cycle for 50 W RF input power, 2 kHz pulsing frequency and 1.5 lpm gas flow rate.	93
Table 5.1 : V_t , I_t , φ and P_{avg} obtained for He APPJ	115
Table 5.2: Average power and input impedance of plasma discharge at APPJ terminals.....	118
Table 5.3: Plasma density (n) of the helium and argon plasma jet for various RF input power.....	140
Table 5.4: Rate of plasma and power flowing out of the annular and central regions	141
Table 5.5: Gas temperature at the glass tube exit of the helium and argon plasma jet.....	142
Table 5.6: Comparison of average gas temperature from model and thermocouple	136

List of Abbreviations

APPJ: Atmospheric Pressure Plasma Jet

CW: Continuous Wave

DBD: Dielectric Barrier Discharge

FWHM: Full Width Half Maximum

MN: Matching Network

OAM: Orbital Angular Momentum

OES: Optical Emission Spectroscopy

PM: Pulse Modulation

QCW: Quasi-Continuous Wave

RF: Radio Frequency

RONS: Reactive Oxygen and Nitrogen Species

List of Notations

- A : Measure of the plasma density
- c_p : Specific heat of the gas per unit mass
- C_L : Load capacitance
- C_T : Tune capacitance
- C_V : Variable capacitance
- d : Spacing between the electrodes
- D : Duty cycle
- D_s : Diffusion coefficient
- D_a : Ambipolar diffusion coefficient
- e : Electronic charge
- E : Electric field
- E_p : Energy content per pulse
- f : Excitation frequency
- f_p : Modulation frequency
- i : Ion
- I_m : Current measured using the I-probe
- I_p : Current measured at APPJ
- I_t : True current
- J_0 : Bessel functions of 1st kind and order zero
- J_1 : Bessel functions of 1st kind order one
- \vec{K} : Propagation constant
- K_B : Boltzmann constant
- K_{mi} : Ion-neutral collision rate constant
- l_1 : Length of electrode overlap region (Region I)
- l_2 : Length of the downstream region (Region II)
- l : Total length of Region I and Region II

L_m : Inductor of Matching network
 L_{ext} : Inductor of LC series resonance circuit
 m : Mass of the electron
 M : Mass of the ion
 n : Plasma density
 n_e : Electron density
 n_i : Ion density
 n_g : Neutral gas density
 n_{sh} : Sheath edge density
 N : Number of helical turns
 p : Pressure
 P : RF input power
 P_{avg} : Average RF input power in pulse modulation mode
 P_{av} : Average power absorbed by the plasma
 $P_{z(0-r_2)}$: Power flowing out of the central region
 $P_{z(r_1-r_2)}$: Power flowing out of the annular region
 Q : Gas flow rate
 r : Radial coordinate
 R : Radial function of plasma density
 r_1 : Radius of the inner electrode
 r_2 : Inner radius of the glass tube
 R_p : Plasma resistance
 R_e : Reynold's number
 s : Sheath width
 T : Total pulse duration
 T_{on} : "on" duration of RF pulse
 T_{off} : "off" duration of RF pulse

T_e : Electron temperature
 T_{exc} : Electron excitation temperature
 T_i : Ion temperature
 T_g : Gas temperature
 T_{g0} : Initial gas temperature
 T_{gl} : Gas temperature at the glass tube exit
 $T_{gl(avg)}$: Gas temperature at the glass tube exit in pulse modulation mode
 T_{r1} : Plasma ejection rate from the annular region
 T_{z1} : Plasma ejection rate from the central region
 U_B : Bohm velocity
 u_g : Gas flow velocity
 V_b : Breakdown voltage
 V_m : Voltage measured using the V -probe
 V_p : Voltage measured at APPJ
 V_t : True Voltage
 \bar{V} : DC self-bias voltage
 w : length of the two wire transmission line
 Y_0 : Bessel functions of 2nd kind and order zero
 Y_1 : Bessel functions of 2nd kind and order one
 z : Axial coordinate
 Z : Axial function of plasma density
 Z_d : Test load impedance
 Z_I : Current probe impedance
 Z_o : Oscilloscope impedance
 Z_p : Plasma impedance
 Z_V : Voltage probe impedance

Greek letters Used

β_l : Phase constant of two-wire transmission line

ΔT_g : Gas heating/change in the gas temperature

ϵ_p : Plasma dielectric constant

Γ_s : Particle flux

Γ_a : Ambipolar flux

Γ_r : Radial flux

Γ_z : Axial flux

λ : Helical pitch

μ : Mobility

ν_m : Electron- neutral momentum transfer frequency

ν_{mi} : Ion-neutral momentum transfer frequency

ν_{iz} : Ionization frequency

φ : Phase difference between voltage and current

ρ : Mass density of the neutral gas

ρ_V : Reflection coefficient

ν : Dynamic viscosity

ω_p : Plasma Frequency